Integrated three-color organic light-emitting devices

C. C. Wu, J. C. Sturm,[a] and R. A. Register
Advanced Technology Center for Photonic and Opotoelectronic Materials (ATC/POEM), Princeton University, Princeton, New Jersey 08544

M. E. Thompson
Department of Chemistry, University of Southern California, Los Angeles, California 90089

(Received 5 August 1996; accepted for publication 12 September 1996)

We report a demonstration of the integration of individual polymer-based light emitting devices of three different colors on the same substrate. Orange, green, and blue color devices are sequentially fabricated on the same indium–tin oxide (ITO) coated glass substrate coated with a patterned insulator on the ITO, by the spin coating of polymer thin films, the vacuum deposition of top metal contacts, and the patterning of polymer thin film by plasma etching, using the top metal contacts as the self-aligned etching mask. The devices exhibit no degradation of device characteristics due to the integration processing compared to discrete devices on separate substrates. This demonstration shows a new path towards the fabrication of high performance low-cost full-color organic flat panel displays. © *1996 American Institute of Physics.* [S0003-6951(96)00547-5]

A long sought goal in the display field has been the integration of light emitting devices (LEDs) of three different colors onto a single substrate. While organic LEDs (OLEDs) have shown extreme versatility in terms of colors and freedom of substrates in recent years,[1–9] integration of OLEDs of different colors has proven difficult because of difficulties associated with the processing and patterning of the organic materials. Therefore, multicolor work to date in the field has been based on integrating red, green, and blue filters over a single type of white emitting device,[9] integrating red and green down-conversion phosphors with a single type of blue emitting device,[10] or adjusting the emission of a single type of broadband organic emitter by using three different kinds of microcavities.[11]

To reach maximum power efficiency for a display, however, the first two of the above three approaches have inherent limitations. A clearly desirable alternative would be to fabricate three different devices with three different organic layers, each optimized for different colors and integrated onto a common substrate. However, the integration of red, green, and blue devices for the subpixels of a full-color display and the microfabrication of small pixels in high resolution displays will definitely involve the patterning of films and microprocessing, which inevitably require the use of solvents, acid, and water. The direct exposure of organic materials to solvents and water can lead to the degradation or even complete failure of devices. In this letter, we demonstrate such integration of three different polymer-based organic LEDs on a single substrate, with each consisting of a different organic layer for a different color.

The general structure of OLEDs consists of a glass substrate, ITO (a transparent conductor), the organic layers, and a patterned top metal contact. The device emits light out of the bottom of the ITO coated glass substrate, and in virtually all devices to date only the top metal contact or the bottom ITO contact has been patterned to define the area of the device, not the organic layer. The integration of devices with different organic layers onto a common ITO layer would involve patterning the organic layers as well. A straightforward integration approach is to sequentially fabricate different sets of devices by preparing the metal contact on each organic layer and then patterning the organic layer to form a patterned device before processing with the next layer of organic materials. The final structure of such an approach is shown in Fig. 1(a). This approach leaves the organic layer exposed on the device edge, where it may be attacked by water, solvents, etc., during later processing. For example, in the integration of polymer-based devices, the spin coating of a second polymer after the completed fabrication of a first device, e.g., the leftmost device in Fig. 1(a), would lead to degradation of the existing device, because the solvent carrier in the second spin-coating step would dissolve the first polymer through the device sidewall. With this approach, we indeed observed irregular shorting, leakage, and degradation of existing devices caused by the attack of solvents through

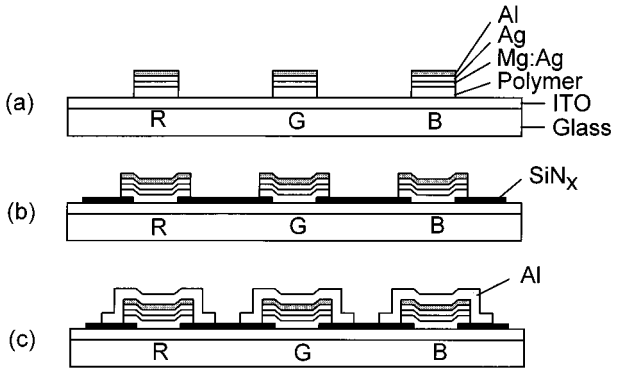

FIG. 1. Cross sections of three integration schemes. The indium–tin–oxide (ITO)-coated glass substrate has a sheet resistance of 10 Ω per square. The magnesium to silver ratio of the magnesium–silver alloy in the cathode is ~10:1; (a) A straightforward integration scheme with only the patterning of organic films; (b) an integration scheme with a patterned insulator on the ITO. The sizes of the active regions and the metal contacts are 2 mm×2 mm and 4 mm×4 mm, respectively; (c) an integration scheme with a patterned insulator on the ITO and a metal sealing layer over each device.

[a]Electronic mail: sturm@ee.princeton.edu

the unprotected device sidewalls, though macroscopically the devices still looked the same.

To overcome this problem, we then rendered the exposed edge of the device electrically inert using a second structure as shown in Fig. 1(b). In this structure, a thin insulating layer is deposited on top of ITO and the active device regions are defined by opening windows on the insulating layer to access the ITO. The use of the insulating layer allows the top metal contacts to extend out of the active areas and leave some distance between the edge of the metal coverage and the actual electrically active region. This strategy successfully keeps the active regions intact in following polymer coating and leaves device characteristics unchanged. The devices work well in dry nitrogen atmosphere, but to prevent any possible attack of the organic materials by air, moisture, or processing liquids through the edge of the device, a refined structure as shown in Fig. 1(c) has also been fabricated. After the etching of each polymer thin film and before the coating of the next polymer, a thick layer of air-stable metal, like Al in our case, is deposited to seal the whole device. Note that except for the difference in ways of organic deposition, all the above schemes can in principle be applied to OLEDs based on molecular organic materials in addition to polymer-based OLEDs reported here.

The details of processing are now described. First, a thin layer of insulating silicon nitride SiN_x of ~1000 Å is deposited on top of cleaned ITO by plasma-enhanced chemical vapor deposition (PECVD) at 250 °C. The active device windows in the SiN_x are then patterned by photolithography and standard etching procedures. The polymer thin film for the first set of devices, which are orange in our case, is then spin-coated to cover the whole surface. Due to the unique way of coating polymer thin film from solution and its macromolecular structure, the polymer thin film formed on the patterned surface is expected to be rather conformal. After spin coating, the top metal contacts for the first set of devices are thermally evaporated through a shadow mask in vacuum $\sim 10^{-6}$ Torr. The metal contact has three layers in stack, with ~500 Å coevaporated Mg:Ag alloy overcoated by ~500 Å silver and ~1000 Å aluminum. The structure is then exposed to an oxygen plasma, which etches away photoresist and organics where exposed, but does not etch the aluminum layer or any layers underneath. Therefore, this plasma etching is self-aligned and does not need an extra mask. Also, the use of dry etching avoids the risk of excessive exposure of the organic films to solvents used in wet etching. If the structure of Fig. 1(c) is applied, the evaporation of aluminum seal for the first set of devices is then performed through another shadow mask before the spin coating of the polymer thin film for the next set of green devices. The steps from spin coating to the evaporation of aluminum seal are then repeated to finish the integration of devices. Except for the transfer of samples to the plasma etching system, all of the polymer processing and evaporator loading is carried out in glove boxes filled with dry nitrogen. In the above processing, the patterning of all metal layers is done by mechanical alignment of shadow masks for metal evaporation for our array of 2 mm by 2 mm devices. Eventually, to make a high-resolution display containing a large array of small devices of at most several hundred microns, the patterning of metal layers by photolithography and etching will probably be required. Such processes are currently under development in our lab.

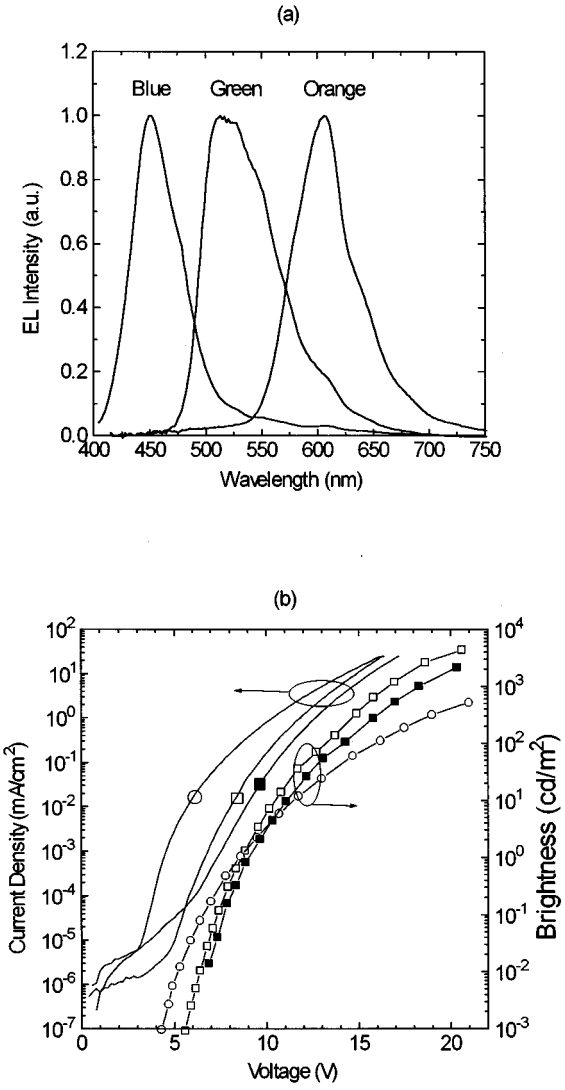

FIG. 2. (a) EL spectra of the orange, green and blue LEDs; (b) forward current–voltage and brightness–voltage characteristics of the orange (open square), green (solid square), and blue (open circle) devices. The compositions of the orange, green, and blue LEDs are ITO/PVK:A1Q:nile red (100:40:0.2)/Mg:Ag, ITO/PVK:A1Q:coumarin 6 (100:40:1.0)/Mg:Ag, and ITO/PVK:PBD:coumarin 47 (100:30:1.0)/Mg:Ag, respectively. The ratios between organic materials are weight ratios and typical organic film thickness are ~1000–1100 Å. A positive voltage is applied to ITO relative to top metal contacts under forward bias.

The devices used in this demonstration are made from molecularly doped polymers (MDP), in which the hole-transporting matrix polymer poly(*N*-vinylcarbazole) (PVK) is doped with electron-transporting molecules, such as tris(8-hydroxy quinolate) aluminum (Alq) or 2-(4-biphenyl)-5-(4-tert-butyl-phenyl)-1,3,4-oxadiazole (PBD) and different fluorescent dyes as efficient emission centers. This class of devices has the advantage that all carrier transport and emissive materials are mixed together in a solution and can be deposited by a single coating step, without the need to address the solvent compatibility of separate carrier transport and emissive layers, simplifying the fabrication. In addition, the emission color can be easily tuned by doping with dif-

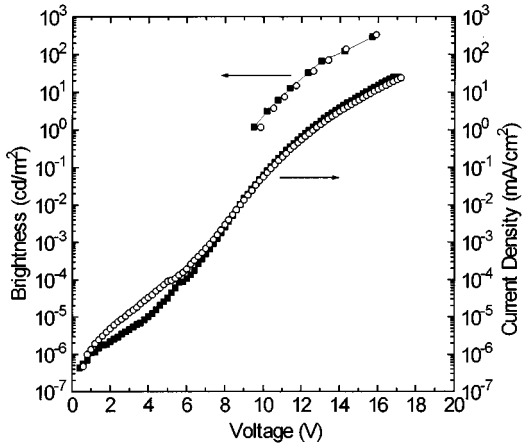

FIG. 3. Brightness–voltage and current–voltage characteristics of the same orange device in the structure of Fig. 1(b) before (solid square) and after (open circle) integration processing.

ferent dyes, and the optical and electrical properties can usually be optimized by tailoring the ratios of different components in MDP. The orange, green, and blue MDPs used in this work are composed of PVK/Alq/nile red, PVK/Alq/coumarin 6, and PVK/PBD/coumarin 47, respectively. The concept of mixing molecular dyes with hole and electron transport materials in a single blend has been demonstrated before,[12–14] but this is the first time our choices of combinations of materials has been reported. Red emission instead of orange emission can be achieved by increasing the nile red fraction, but with loss of efficiency. The electroluminescence spectra of the three devices are shown in Fig. 2(a). Typical $I-V$ characteristics are shown in Fig. 2(b), along with the brightness versus voltage curves ($L-V$). The external quantum efficiencies, measuring only light through the back of the glass substrate, were 0.7%, 0.5%, and 0.4% photon/electron for orange, green, and blue, respectively. Although not record results for single devices, practical brightnesses can be obtained at reasonable operating voltages, for example, video brightness ~100 cd/m^2 at 11–13 V and high brightness ~4000 cd/m^2 around 20 V. The effect of integration processing on devices was checked by comparing the characteristics of devices when they were just freshly made to those of the same devices after they underwent all integration processing. Figure 3 compares the $L-V$ and $I-V$ curves of an orange device in the structure of Fig. 1(b) before and after the integration processing, which in this case means two spin-coating steps and two oxygen plasma etching steps. The device characteristics are unchanged after integration processing, as seen in Fig. 3, and are virtually identical to those of discrete devices as shown in Fig. 2. The plasma etching step was found to be especially benign. Devices subjected to plasma etching without the patterned insulator as shown in Fig. 1(a) also exhibited no visible change compared to their operation before the organic material was patterned. Finally, a color photo of the integrated orange, green, and blue devices all operating simultaneously in the air under the illumination of an incandescent lamp is shown in Fig. 4.

In summary, we have successfully demonstrated the integration of individual polymer-based OLEDs with different organic layers onto a single substrate. The integrated orange, green, and blue devices on the same substrate show no degradation compared to discrete devices. This integration may be a significant step towards the realization of high efficiency full-color organic flat panel displays.

The support of the ATC/POEM at Princeton is gratefully acknowledged.

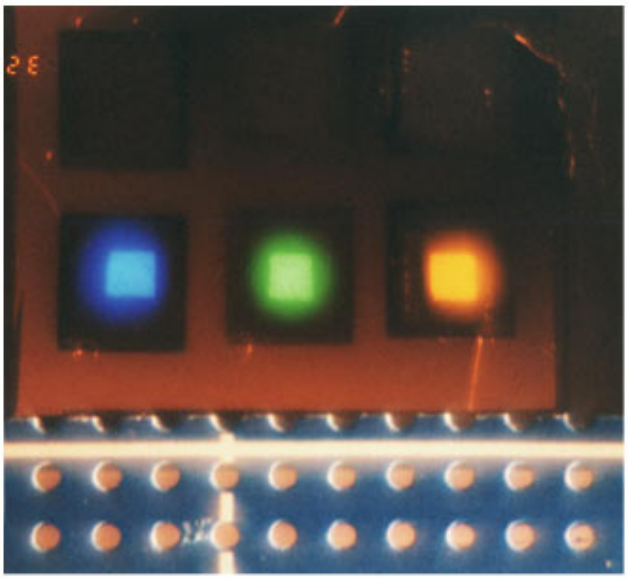

FIG. 4. A color photograph of working integrated orange, green, and blue devices with the structure of Fig. 1(c). The photo was taken in the air under the illumination of a regular 60 W incandescent lamp. The exposure time was 1/60 s and the brightness of the orange, green, and blue devices were ~100, ~100, and ~60 cd/m^2, respectively.

[1] C. W. Tang and S. A. VanSlyke, Appl. Phys. Lett. **51**, 913 (1987).
[2] C. W. Tang, S. A. VanSlyke, and C. H. Chen, J. Appl. Phys. **65**, 3610 (1989).
[3] C. Adachi, S. Tokito, T. Tsutsui, and S. Saito, Jpn. J. Appl. Phys. **27**, L269 (1988).
[4] J. H. Burroughes, D. D. C. Bradley, A. R. Brown, R. N. Marks, K. Mackay, R. H. Friend, P. L. Burns, and A. B. Holmes, Nature **347**, 539 (1990).
[5] D. Braun and A. J. Heeger, Appl. Phys. Lett. **58**, 1982 (1991).
[6] G. Gustafsson, Y. Cao, G. M. Tracy, F. Klavetter, N. Colaneri, and A. J. Heeger, Nature (London) **357**, 477 (1992).
[7] G. Grem, G. Leditzky, B. Ullrich, and G. Leising, Adv. Mater. **4**, 36 (1992).
[8] N. C. Greenham, S. C. Moratti, D. D. C. Bradley, R. H. Friend, and A. B. Holmes, Nature (London) **365**, 628 (1993).
[9] J. Kido, M. Kimura, and K. Nagai, Science **267**, 1332 (1995).
[10] C. W. Tang, D. J. Williams, and J. C. Chang, U.S. Patent No. 5, 294, 870 (1994).
[11] A. Dodabalapur, L. J. Rothberg, and T. M. Miller, Electron. Lett. **30**, 1000 (1994).
[12] J. Kido, M. Kohda, K. Okuyama, and K. Nagai, Appl. Phys. Lett. **61**, 761 (1992).
[13] J. Kido, H. Shionoya, and K. Nagai, Appl. Phys. Lett. **67**, 2281 (1995).
[14] G. E. Johnson, K. M. McGrane, and M. Stolka, Pure & Appl. Chem. **67**, 175 (1995).